Eur. Phys. J. D (2017) 71: 283
DOI: 10.1140/epjd/e2017-80295-2

THE EUROPEAN PHYSICAL JOURNAL D

Regular Article

Cross sections and transport coefficients for H_3^+ ions in water vapour*

Vladimir Stojanović[1,a], Zoran Raspopović[1], Jasmina Jovanović[1,2], Željka Nikitović[1], Dragana Marić[1], and Zoran Lj. Petrović[1,3]

[1] Centre for Non-Equilibrium Processes, Institute of Physics, University of Belgrade, POB 68, 11080 Belgrade, Serbia
[2] Faculty of Mechanical Engineering, University of Belgrade, Kraljice Marije 16, 11000 Belgrade, Serbia
[3] Serbian Academy of Sciences and Arts, Knez Mihailova 35, 11000 Belgrade, Serbia

Received 30 April 2017 / Received in final form 14 August 2017
Published online 14 November 2017 –

Abstract. Scattering cross sections for positive H_3^+ ions in water vapour were calculated by a simple but quite general theory and then assessed by using the available data. Transport coefficients for H_3^+ ions in water vapour in DC fields were calculated by using a Monte Carlo simulation from low to moderate reduced electric fields E/N (E is electric field and N is gas number density) where the non-conservative collisions are also taken into account.

1 Introduction

Plasmas are already deeply incorporated into our everyday life either directly or indirectly within production technologies that are superior to other production methods. Plasma technologies offer treatment of various substances [1–3]. Control of reactive ion plasmas is necessary in applications related to semiconductor modifications. A cornerstone in modelling of such plasmas is precise information on the transport of ions, as the reactive ions flux and energy control the surface processes. In plasmas in collision-dominated regimes, if the negative ions dominate over the electrons, the plasmas become electronegative with properties distinctly different from the electropositive plasmas, especially in the sheath regions. In modelling and analyzing of the plasma chemistry, the cross-sections are needed (rather than interaction potentials) for all relevant species and not only concerning the momentum transfer.

In order to control increasingly complex plasmas large databases for positive and negative ion transport properties are required [4,5]. Databases should be constantly updated with new and improved data [6]. Apart from a wide range of data produced up to now in the field of ion-molecule collisions, there are still major gaps in cases of very reactive gases such as BF_3 that are not convenient to study experimentally. There are also very complex environments such as water vapor where very sophisticated methods are needed in order to obtain some information. Sets that include cross sections for reactive processes are needed to calculate the chemical kinetics of all the species when some of the species may have low density but also have a narrow range of processes controlling their population. To remedy lack of data simpler theories have been used and in this paper we exploited so-called Denpoh and Nanbu (DN) model [7], together with other techniques to make reasonable estimates of the ion scattering cross sections. In addition to cross sections, reaction rates [8] and other transport data may be used directly in fluid and hybrid codes and in process of normalization of cross sections. An important aspect of plasma models is that a complete set of cross sections should be used. Otherwise, even if one had all perfect cross sections albeit with an incomplete set, the results would be unrealistic.

In this paper Monte Carlo technique was applied to perform calculations of transport parameters, as well as of rate coefficients in DC electric fields. We have used a Monte Carlo code that properly calculates collision probabilities for thermal collisions [9]. The code has passed all the relevant benchmarks [9] and has been tested in our work on several types of charged particles [10,11]. The choice of three seemingly different molecules with different improvements is intended as a review of the approach in supplementing the existing data with simple theories and basic calculations.

2 Cross sections

Ion-molecule reactions play a basic role in the field of gas phase reaction kinetics. They are readily studied over a wide range of collision energies and the ionic reactants in a number of cases can be prepared in defined excited

* Contribution to the Topical Issue "Physics of Ionized Gases (SPIG 2016)", edited by Goran Poparic, Bratislav Obradovic, Dragana Maric and Aleksandar Milosavljevic.

[a] e-mail: stoyanov@ipb.ac.rs

states (see for example Ref. [12]). There is a very detailed knowledge of the ion molecule reactions in general in the literature. Nevertheless, concerning the cross sections that are necessary for modelling plasma processing there is a shortage of data even for the most pertinent processes and therefore a considerable effort in extending the existing databases is required.

At low collision energies (thermal to few electron volts) activated complex formation usually dominates the outcome of the collisions. For pressures in low temperature plasmas, related to technological applications, ranging up to atmospheric pressure average flight time between collisions is more than 4 orders of magnitudes larger than the average lifetime of activated complex [13,14]. Having that in mind the reaction can be safely assumed as infinitesimally short both in space and time. Since a large proportion of near-thermal ion-molecule reactions proceed without significant barriers, statistical theories of unimolecular decay have been successful in reproducing low-energy ion-molecule reaction rates, as well as the product state distributions [15].

Rice-Ramsperger-Kassel (RRK) theory of unimolecular reactions has proven to be not only a cornerstone for more precise theories that include quantum effects such as RRKM [16,17] but is also a sufficiently reliable method to be used to explain measurements of the rate constants (subject to selecting the required empirical parameters [18]).

Denpoh and Nanbu [7] obtained reactive cross sections for ions in collision with molecular gas by assuming their behavior close to target is affected only by the induced polarisation potential. For ions in low pressure Ar/CF_4 RF discharges they included all possible reactions with CF_4 molecule and calculated thermodynamic thresholds in the energy region about 10 times wider than the expected validity of the induced polarisation potential. They separated elastic from reactive endothermic collisions and determined branching ratio according to RRK theory which is used to calculate the scattering probability for each reaction. In their approach each reaction cross section is proportional to the scattering probability normalized to appropriate total cross section [7]. Assuming that each binary collision produces reaction with the activated complex formation, as a total cross section for reactions they used orbiting cross section [19] multiplied by cut-off value of normalized impact parameter β_∞^2 [7,20]. In terms of classical trajectory analysis [19] this means that reactions proceed within scaled orbiting distance $b_0\beta_\infty$, where the internal energy of the complex in RRK analysis is equal to the initial kinetic energy of the particles in the center of mass system. In their approach usage of normalized impact parameter allows one to calculate angles of scattering and subsequently velocities of particles after the scattering.

In this work we exploit DN model to calculate the complete cross section set for scattering of H_3^+ ions on H_2O molecules. Our basic assumption is that all trajectories appearing within orbiting distance may lead to reactions [19] while trajectories not entering the orbiting distance are leading to anisotropic elastic scattering.

We have used Monte Carlo simulations (MCS) to calculate transport parameters [8]. In order to calculate the total collision frequency in MCS we have employed the total momentum transfer cross section [21].

The basis of standard RRK theory is that critical motion leading to the chemical reaction of a molecule is vibrational. It is assumed that molecule is a collection of s classical oscillators where one of these oscillators is critical to the reactions. It is necessary to adjust number of vibrational modes by using a factor $1/n$ where the choice of n at the first instance apparently involves some degree of intuition. It is found empirically that the best agreement with experimental measurements of rate constants, for the widest range of cases is achieved for n equal to about 2 [22–24].

Number of endothermic processes that are included in DN model becomes important if possibly missing processes have threshold in the range of validity of the polarization interaction. Since consistent tables of thermochemical data are readily available [25] for large number of reactions it is possible to calculate the thermodynamic thresholds. On the other hand, we may choose to neglect processes with higher thresholds especially if ions seldom reach such energies.

Large dipole moments of gas particles significantly affect the ion-molecule interaction and increase reaction cross section. Stojanović et al. [26] used DN model for scattering O^- ions in water vapor. They calculated cross sections by using the locked dipole approximation [20]. Obtained cross section set was than corrected to fit the reduced mobility calculated by the SACM (Statistical Adiabatic Channel Model) approximation [27]. Those calculations proved to be in good agreement with the existing experimental measurements. In general DN model may be used on its own as a source of data especially when results from experiments and/or binary collision theories of a higher order are not available. We choose to combine the model with the swarm procedure to test the cross section sets. There we employ as many experimental data as available to improve the accuracy of results for cross sections and consequently for transport coefficients.

In this work we present the cross section set for $H_3^+ + H_2O$ calculated by the same method. For presented cross section set we have selected 24 endothermic reaction paths and one exothermic reaction. In calculations, we have assumed that effective number of vibrational modes is 6. Ratio between total momentum cross section and orbiting cross section is used as for the case where dipole moment of the target is neglected. Finally, exothermic reaction cross section is obtained by scaling reduced orbiting cross section according to experimentally obtained rate coefficient for the exothermic reaction. H_3^+ is in-avoidable molecule in studies of low pressure and astrophysical plasmas. It is known that H_3^+ is produced in astrophysical plasmas, in exothermic reactions of H_2^+ with H_2 [28]. Note (see Tab. 1) that the same internal energy if transferred to H_3^+ in collisions with water only increases exothermicity and cannot produce other particles than again H_3O^+ (process 2).

Table 1. H_3^+–H_2O reaction paths products and the corresponding thermodynamic threshold energies Δ.

No	Reaction products	Δ (eV)
1(EL)	$H_3^+ + H_2O$	0
1(EXO)	$\mathbf{H_3O^+ + H_2}$ **(EXO)**	2.8097
2	$H_3O^+ + 2H$	−1.6676
3	$H_2O^+ + H + H_2$	−3.3465
4	$H_2O^+ + 3H$	−7.8238
5	$H_3^+ + H_2 + O$	−5.0587
6	$H_3^+ + 2H + O$	−9.5359
7	$H_3^+ + OH + H$	−5.1126
8	$H_2^+ + H_2O + H$	−6.1904
9	$H_2^+ + H + H_2 + O$	−11.249
10	$H_2^+ + 3H + O$	−15.726
11	$H_2^+ + 2H + OH$	−11.303
12	$H_2^+ + H_2 + OH$	−6.8257
13	$H^+ + H_2O + H_2$	−4.3632
14	$H^+ + H_2O + 2H$	−8.8405
15	$H^+ + H_2 + O + 2H$	−13.899
16	$H^+ + H_2O + 2H$	−9.4219
17	$H^+ + 4H + O$	−18.376
18	$H^+ + OH + H_2 + H$	−9.4758
19	$H^+ + OH + 3H$	−13.953
20	$O^+ + 2H_2 + H$	−9.4416
21	$O^+ + 3H + H_2$	−13.919
22	$O^+ + 5H$	−18.396
23	$OH^+ + 2H_2$	−4.4006
24	$OH^+ + 2H + H_2$	−8.8778
25	$OH^+ + 4H$	−13.355

3 Calculation of transport parameters

H_3^+ is not an important molecular ion in water vapor discharges but is contributing to production of H_3O^+ molecule which has been shown to be the most abundant in water vapor discharges and also in other discharges where water can be present either as a part of the mixture or as impurity. Since experimental rate coefficient for H_3O^+ production exist at thermal energies, we have used these data to normalize the reduced orbiting cross section [19] and thus improve uniqueness of the obtained cross section set. Product distributions for those reactants are found not dependent on amount of vibrational excitation of H_3^+ [29] thus only endothermic reactions may have slightly shifted thresholds towards low energy while number of reactive channels will remain the same as with H_3^+ in ground state.

Cross sections were calculated by applying DN model for scattering of H_3^+ on H_2O with the same data for polarizability and dipole moment of H_2O as used by Clary [30] and selected heats of formation from reference [25]. In Table 1 we show reaction paths products and the corresponding thermodynamic threshold energies.

Cross section set that includes differentiation of elastic and exothermic process (EXO) is shown in Figure 1. While most inelastic channels occur at high energies beyond the standard energies for gas discharges, there are some processes taking place with thresholds in the vicinity of 2–4 eV that may become relevant for most discharges.

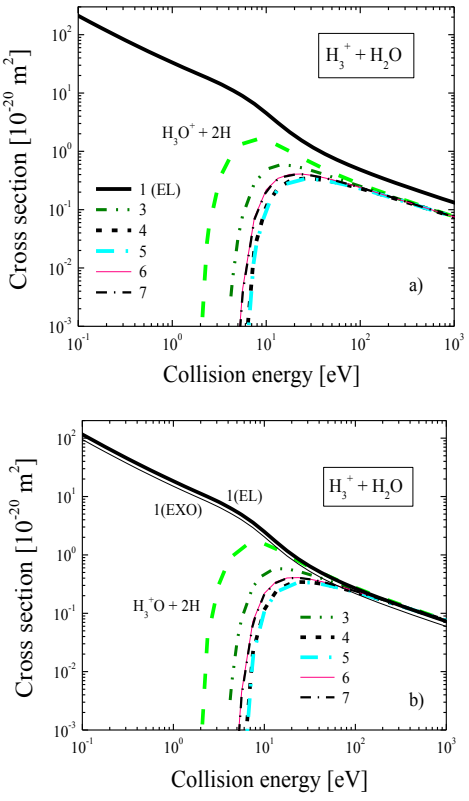

Fig. 1. Cross section set for $H_3^+ + H_2O$ scattering: (a) without the non-conservative effect of the exothermic collisions, (b) with the non-conservative effect of the exothermic collisions. Only endothermic processes with thermodynamic thresholds lower than 6 eV are included in this figure but we have cross sections for all processes from Table 1.

Exothermic processes are often disregarded in their non-conservative nature, and simply added to the total elastic cross section. In any case, all channels will be accessible in the sheath of the discharge.

Regarding elastic and exothermic processes one can differentiate between two situations. In the first case one can add 1(El) and 1(EXO) processes (Fig. 1a) and treat the process as elastic. Thereby one neglects the number-changing nature of the exothermic process. If exothermic reaction with products $H_3O^+ + H_2$ is included as a non-conservative loss (Fig. 1b) then it may affect the calculated transport data greatly. We have normalized the exothermic cross section to the thermal rate at $T = 297$ K [31] and thus also scaled the total momentum transfer cross section [32].

The cross section for exothermic collisions σ_{exo} is introduced by

$$\sigma_{exo} = \beta \cdot \sigma_O \tag{1}$$

where σ_O is the orbiting cross section and β is the scaling factor. Scaling factor can be determined if the thermal rate constant for exothermic process is available. For the case of $H_3^+ + H_2O$, rate coefficient at $T = 297$ K for exothermic reaction with products $H_3O^+ + H_2$ is measured by Betowski et al. [31] and it gives $\beta = 0.4498$ [1]. Note that

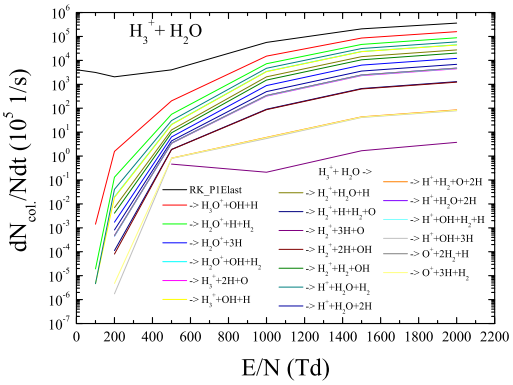

Fig. 2. Rate coefficients for reactions of H_3^+ ions with H_2O at $T = 300$ K, calculated by Monte Carlo simulations. The results were obtained without the non-conservative effect of the exothermic reaction.

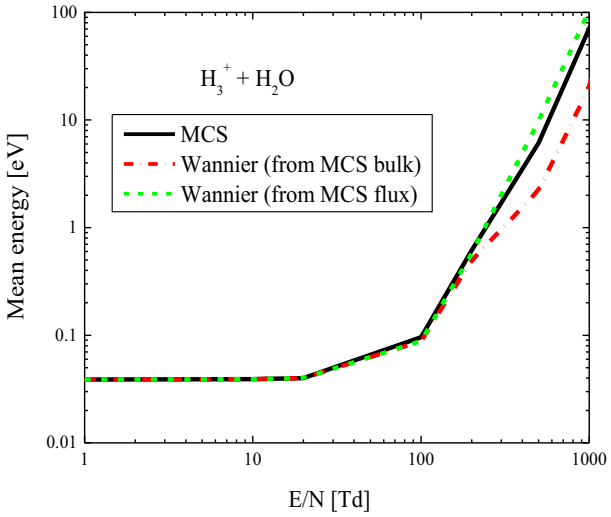

Fig. 3. Mean energy obtained from simulations and also from Wannier relations [32]. Two different drift velocities (bulk and flux see [34]) were used for Wannier relations.

our cross section for exothermic collisions has the same energy dependence as the reduced orbiting cross section obtained for the case of potential with dipole and induced polarization term.

The obtained cross section set was corrected to fit the reduced mobility calculated by SACM approximation [29], i.e. the zero field mobility of $Ko = 1.7795$ cm^2 V^{-1} s^{-1} at $T = 300$ K. We calculated rate coefficients (see Fig. 2) for reactions shown in Table 1 by using MCS. Under the same circumstances, we have obtained the mean energy and compared it with the predictions based on Wannier relations [32] using the cross sections from the MCS. Those results are shown in Figure 3. The difference between the bulk and flux drift velocities is a consequence of the energy-dependent endothermic reactions [33,34]. Strong dipole forces cause discrepancy of collisional frequency from constant value characteristic for transport of ions in the induced polarization potential [35]. In principle we are here testing the Wannier relations, but more importantly we are using in the relation the two varieties of the drift velocities (flux and bulk). The idea is to see which provides a better estimate of the mean energy, as non-conservative processes were not included explicitly in the development of these relations. Since non-conservative effect of the exothermic relation is huge, we chose to make this comparison by using only the endothermic non-conservative processes such as ionization. We can see that the predictions of Wannier relations using the flux drift velocity are in a much closer agreement with the mean energy obtained in the same simulation.

4 Transport under the influence of a strong non-conservative exothermic process

Exothermic collisions cause differences between flux and bulk drift velocities at low E/N while endothermic reactive collisions affect the swarm at high E/N. The former, however affects the transport on a much larger scale due to a larger cross section and also as it occurs in the energy region of the bulk of most gas discharges. On the other hand, if collision frequency of exothermic collisions is constant that results in equality of the bulk and flux reduced mobilities since the ions from the front and the tail are removed with an equal rate [34].

In order to indicate the importance of including the nature of all processes we have compared calculations of transport coefficients with and without the non-conservative effect of exothermic process or in other words when losses of transported ions are taken into account or when (as is usually the case in simpler models) those processes are included by their number in the total cross section. As for the isotropic scattering elastic and momentum transfer cross sections are the same this process is then effectively added to the elastic process. The calculated transport coefficients are shown in Figure 4.

At low mean energies due to energy dependence of the collision rates one has "heating" of the swarm due to preferential removal of the low energy particles. This results in a greater bulk drift velocity. When reduced electric field further increases, energy distribution of the ions becomes wider and number of slow ions that are removed by exothermic reactions reduces, so the bulk drift velocity approaches flux drift velocity. Bulk drift velocity becomes lower than flux drift velocity when endothermic collisions begin to dominate. Reactive collision frequency due to the endothermic collisions increases with respect to constant collision frequency and one has swarm "cooling" due to a preferential loss at higher energies.

In our case, bulk drift velocity appears as slowly varying function of E/N up to about 300 Td. At that point it becomes equal to the flux velocity and later on it becomes smaller. Behaviour of the diffusion coefficients is quite different due to tremendous effect of cooling and heating of the distribution function on the diffusion.

5 Conclusion

In this work we present details of how Denpoh-Nanbu model is used to calculate cross sections for reactive scattering of H_3^+ ions with H_2O target for energies in the range

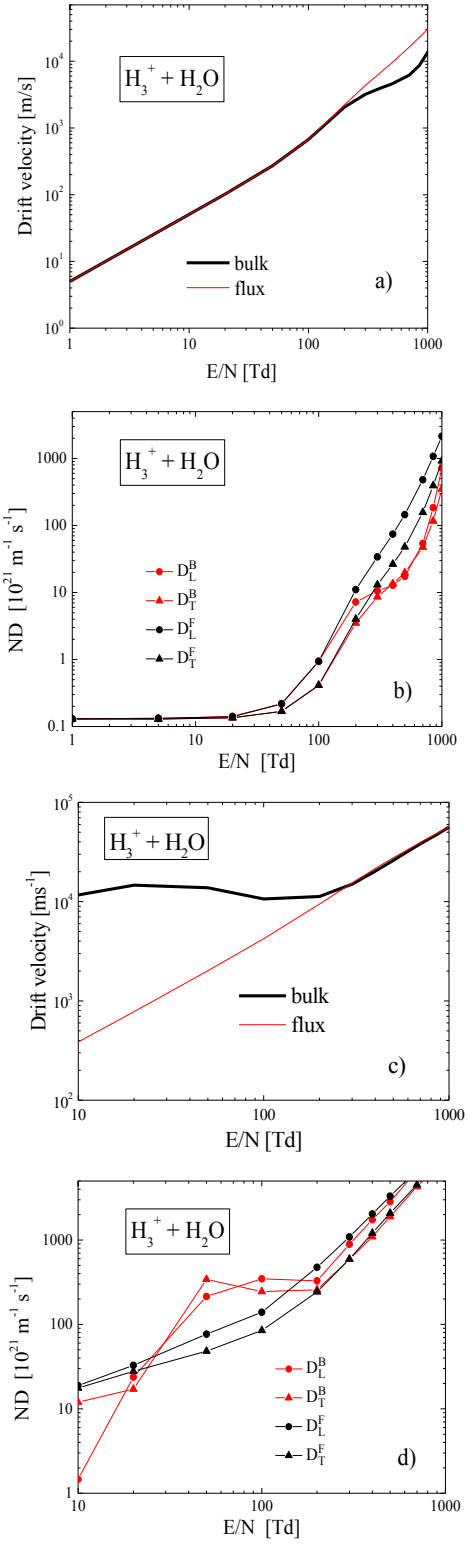

Fig. 4. Transport parameters as a function of E/N for H_3^+ in H_2O, exothermic losses not included: (a) drift velocity, (b) diffusion coefficients; exothermic losses included, (c) drift velocity, and (d) diffusion coefficients.

from 0.01 eV to 200 eV. The role of these ions in water vapour containing discharges is essential especially in the chain of reactions leading to formation of the dominant H_3O^+ ions.

Cross section set and transport parameters presented in this work were not available up to now. Accuracy of exothermic cross section is ±25% that comes from accuracy of the experimental rate constant and having in mind successful description of exothermic reactions by capture theories. Langevin Hasse model provides a good low energy total cross section that may be successfully extrapolated to higher energies. Having in mind the uncertainty of the polarizabilities available in the literature and the tests made for other ions by the same technique the total cross section at lower energies is uncertain to ±20%. Although accuracy of the particular endothermic cross sections may vary significantly, approximate accuracy of data is about ±50% with an uncertainty of the total effect of endothermic inelastic processes being established more accurately.

The Monte Carlo technique was applied to carry out calculations of transport parameters as a function of reduced electric field. Due to the lack of experimental transport data, such calculations for H_3^+ ions in H_2O are the best data that are available. The information on all the reactants is an important part of the kinetic models for discharges in mixtures with water vapour, in the interface between liquid water and air and in the discharges in liquids [36–43].

This work is partly supported by Ministry of Education, Science and Technology of Republic Serbia projects ON171037 and III410011. ZLjP is also grateful to the SASA project 155. This work was also a part of our group's activities within the COST Action TD1208.

Author contribution statement

Vladimir Stojanović – calculation of endothermic and exothermic cross sections, cross section set assessment; organization of input data and graphical presentation. Initial version of the manuscript. Zoran Raspopović – Monte Carlo simulations for cases where exothermic collisions are included. Jasmina Jovanović – Monte Carlo simulations for cases where elastic and endothermic collisions are included. Initial version of the manuscript. Željka Nikitović – enthalpy calculations for all reactants and products. Dragana Marić – coordinator of a program to provide the required data for relevant constituents in water vapour, liquid and heterogeneous liquid gas system discharge modelling. Zoran Lj. Petrović – defining the plan for research and development of the required procedure. Development of the Monte Carlo code used in the paper. Organization and finalization of the manuscript.
All authors have read and approved the final manuscript.

References

1. M.A. Lieberman, A.J. Lichtenberg, *Principles of Plasma Discharges and Materials Processing*, 2nd ed. (Wiley, 2005)
2. T. Makabe, Z. Petrović, *Plasma Electronics: Applications in Microelectronic Device Fabrication* (Taylor and Francis, CRC Press, New York, 2006)
3. Z.Lj. Petrović, P. Maguire, M. Radmilović-Radjenović, M. Radetić, N. Puač, D. Marić, C. Mahony, G. Malović, in *Nanotechnology for Electronics, Photonics and Renewable Energy*, edited by A. Korkin et al. (Springer, 2010), Vol. 85
4. S. Samukawa, M. Hori, S. Rauf, K. Tachibana, P. Bruggeman, G. Kroesen, J.C. Whitehead, A.B. Murphy, A.F. Gutsol, S. Starikovskaia, U. Kortshagen, J.-P. Boeuf, T.J. Sommerer, M.J. Kushner, U. Czarnetzki, N. Mason, J. Phys. D: Appl. Phys. **45**, 253001 (2012)
5. I. Adamovich, S. Baalrud, A. Bogaerts, P.J. Bruggeman, M. Cappelli, V. Colombo, U. Czarnetzki, U. Ebert, J.G. Eden, P. Favia, D.B. Graves, S. Hamaguchi, G. Hieftje, M. Hori, I.D. Kaganovich, U. Kortshagen, M.J. Kushner, N.J. Mason, S. Mazouffre, S. Mededovic Thagard, H.-R. Metelmann, A. Mizuno, E. Moreau, A.B. Murphy, B.A. Niemira, G.S. Oehrlein, Z. Lj. Petrović, L.C. Pitchford, Y.-K. Pu, S. Rauf, O. Sakai, S. Samukawa, S. Starikovskaia, J. Tennyson, K. Terashima, M.M. Turner, M.C.M. van de Sanden, A. Vardelle, J. Phys. D: Appl. Phys. **50**, 323001 (2017)
6. http://mail.ipb.ac.rs/~cep/ipb-cnp/ionsweb/database.htm; www.lxcat.net, see for example Phelps or Viehland database, retrieved on: 2017/04/05
7. K. Denpoh, K. Nanbu, J. Vac. Sci. Technol. A **16**, 1201 (1998)
8. J. Tennyson, S. Rahimi, C. Hill, L. Tse, A. Vibhakar, D. Akello-Egwel, D.B. Brown, A. Dzarasova, J.R. Hamilton, D. Jaksch, S. Mohr, K. Wren-Little, J. Bruckmeier, A. Agarwal, K. Bartschat, A. Bogaerts, J.-P. Booth, M.J. Goeckner, K. Hassouni, Y. Itikawa, B.J. Braams, E. Krishnakumar, A. Laricchiuta, N.J. Mason, S. Pandey, Z.Lj. Petrovic, Y.-K. Pu, A. Ranjan, S. Rauf, J. Schulze, M.M. Turner, P. Ventzek, J.C. Whitehead, J.-S. Yoon, Plasma Sources Sci. Technol. **26**, 055014 (2017)
9. Z. Ristivojević, Z.Lj. Petrović, Plasma Sources Sci. Technol. **21**, 035001 (2012)
10. Z.Lj. Petrović, Z.M. Raspopović, V.D. Stojanović, J.V. Jovanović, G. Malović, T. Makabe, J. de Urquijo, Appl. Surf. Sci. **253**, 6619 (2007)
11. J. de Urquijo, J.V. Jovanović, A. Bekstein, V. Stojanović, Z.Lj. Petrović, Plasma Sources Sci. Technol. **22**, 025004 (2013)
12. C.L. Liao, C.X. Liao, C.Y. Ng, J. Chem. Phys. **81**, 5672 (1984)
13. Y. Xu, B. Xiong, Y.C. Chang, C.Y. Ng, J. Chem. Phys. **139**, 024203 (2013)
14. D.K. Bohme, D.B. Dunkin, F.C. Fehsenfeld, E.E. Ferguson, J. Chem. Phys. **51**, 863 (1969)
15. H.F. Davis, H.U. Stauffer, in *Encyclopedia of Physical Science and Technology*, 3rd ed., edited by R.A. Meyers (Academic Press, 2000), Vol. 4, p. 697
16. R.A. Marcus, J. Chem. Phys. **20**, 359 (1952)
17. H.O. Pritchard, *The Quantum Theory of Unimolecular Reactions* (Cambridge University Press, 1984)
18. D.W. Placzek, B.S. Rabinovitch, G.Z. Whitten, E. Tschuikow-Roux, J. Chem. Phys. **43**, 4071 (1965)
19. E.W. McDaniel, V. Čermak, A. Dalgarno, E.E. Ferguson, L. Friedman, *Ion-Molecule Reactions* (Wiley-Interscience, 1970)
20. J.V. Dugan, J.L. Magee, J. Chem. Phys. **47**, 3103 (1967)
21. Z.Lj. Petrović, V.D. Stojanović, J. Vac. Sci. Technol. A **16**, 329 (1998)
22. D.W. Placzek, B.S. Rabinovitch, G.Z. Whitten, J. Chem. Phys. **43**, 4071 (1965)
23. G.B. Skinner, B.S. Rabinovitch, J. Phys. Chem. **76**, 2418 (1972)
24. H.W. Schranz, S. Nordholm, N.D. Hamer, Int. J. Chem. Kinet. **14**, 543 (1982)
25. S.G. Lias, J.E. Bartmess, J.F. Xebman, J.L. Holmes, R.D. Levin, W.G. Mallard, J. Phys. Chem. Ref. Data **17**, 1 (1988)
26. V. Stojanović, Z. Raspopović, D. Marić, Z.Lj. Petrović, Eur. Phys. J. D **69**, 6 (2015)
27. J.A. de Gouw, M. Krishnamurthy, S.R. Leone, J. Chem. Phys. **106**, 5937 (1997)
28. A.V. Phelps, Phys. Rev. E **79**, 066401 (2009)
29. J.K. Kim, I.P. Theard, W.T. Huntress, Int. J. Mass Spectrosc. Ion Phys. **15**, 223 (1974)
30. D.C. Clary, Chem. Phys. Lett. **232**, 267 (1995)
31. D. Betowski, J.D. Payzant, G.I. Mackay, D.K. Bohme, Chem. Phys. Lett. **31**, 321 (1975)
32. G.H. Wannier, Bell Syst. Tech. J. **32**, 170 (1953)
33. Z.Lj. Petrović, S. Dujko, D. Marić, G. Malović, Ž.D. Nikitović, O. Šašić, J. Jovanović, V. Stojanović, M. Radmilović-Rađenović, J. Phys. D: Appl. Phys. **42**, 194002 (2009)
34. R.E. Robson, Aust. J. Phys. **44**, 685 (1991)
35. Z. Raspopović, V. Stojanović, Ž. Nikitović, EPL **111**, 45001 (2015)
36. P.J. Bruggeman, M.J. Kushner, B.R. Locke, J.G.E. Gardeniers, W.G. Graham, D.B. Graves, R.C.H.M. Hofman-Caris, D. Marić, J.P. Reid, E. Ceriani, D. Fernandez Rivas, J.E. Foster, S.C. Garrick, Y. Gorbanev, S. Hamaguchi, F. Iza, H. Jablonowski, E. Klimova, J. Kolb, F. Krcma, P. Lukes, Z. Machala, I. Marinov, D. Mariotti, S. Mededovic Thagard, D. Minakata, E.C. Neyts, J. Pawlat, Z.Lj. Petrović, R. Pflieger, S. Reuter, D.C. Schram, S. Schröter, M. Shiraiwa, B. Tarabová, P.A. Tsai, J.R.R. Verlet, T. von Woedtke, K.R. Wilson, K. Yasui, G. Zvereva, Plasma Sources Sci. Technol. **25**, 053002 (2016)
37. S.A. Norberg, E. Johnsen, M.J. Kushner, Plasma Sources Sci. Technol. **24**, 035026 (2015)
38. D.X. Liu, P. Bruggeman, F. Iza, M.Z. Rong, M.G. Kong, Plasma Sources Sci. Technol. **19**, 025018 (2010)
39. T. Murakami, K. Niemi, T. Gans, D. O'Connell, W.G. Graham, Plasma Sources Sci. Technol. **22**, 015003 (2013)
40. F. Taccogna, G. Dilecce, Eur. Phys. J. D **70**, 251 (2016)
41. E.R. Adhikari, S. Ptasinska, Eur. Phys. J. D **70**, 180 (2016)
42. S. Lazović, D. Maletić, A. Leskovac, J. Filipović, N. Puač, G. Malović, G. Joksić, Z.Lj. Petrović, Appl. Phys. Lett. **105**, 124101 (2014)
43. A. Hurlbatt, A.R. Gibson, S. Schroter, J. Bredin, A.P.S. Foote, P. Grondein, D. O'Connell, T. Gans, Plasma Process. Polym. **14**, 1600138 (2017)